Model Membranes for the Study of Active Transport Phenomena

W. R. Krigbaum*[1] and Robert A. Majeski

Department of Chemistry, Gross Chemical Laboratory, Duke University, Durham, North Carolina 27706. *Received April 1, 1977*

ABSTRACT: Models for active transport are prepared by the covalent bonding of molecules containing a catalytic site to the membrane asymmetrically with respect to its thickness. The membrane separates two compartments of unequal volume, both initially containing reactant at the same concentration. We observed the time dependence of the reactant and product concentrations, and of the osmotic pressure, and these results are compared with theoretical predictions. The two reactions studied are the hydrolysis of ethyl *N*-acetyl-L-tyrosinate catalyzed by α-chymotrypsin and the acid-catalyzed hydrolysis of triethoxymethane. The asymmetric membrane consumes reactant, and discharges product, at different rates through its two faces. The cencentration of products, and of non-rate-determining reactants, may exhibit maxima or minima with time, and computer simulation indicates that oscillatory behavior could be expected under appropriate conditions. Due to the different exit path lengths, the osmotic response (determined by the solute concentrations at the two membrane surfaces) may be opposite in sign to that expected from the concentrations in the external compartments.

Background

Active transport, a process essential to living organisms, involves the passage of molecules or ions across a membrane in the direction from lower to higher chemical (or electrochemical) potential. The objective of this work is to synthesize model membranes and to investigate their behavior experimentally in order to gain insight into the parameters which affect such transport processes.

Transport of any species against the gradient of its chemical potential is an irreversible process, so that guidance in the design of such model systems must be sought in the thermodynamic treatment of irreversible processes. This makes it evident, for example, that active transport must involve coupled processes, in which the rate of a particular process is conditioned by more than one driving force. In the simplest case of two coupled processes, the rate of internal entropy production, d_iS/dt, can be expressed in terms of generalized flows J and forces X in the following manner:

$$d_iS/dt = J_1X_1 + J_2X_2 \geq 0 \quad (1)$$

Further, if the system is not too far removed from equilibrium, a linear relationship obtains between each flow and its conjugate forces:

$$J_1 = L_{11}X_1 + L_{12}X_2 \quad (2a)$$

$$J_2 = L_{21}X_1 + L_{22}X_2 \quad (2b)$$

The "proper" coefficients, L_{11} and L_{22}, must be positive, while the "mutual" coefficients may be either positive or negative, but they must obey the Onsager-Casimir reciprocity relations. Our interest will be confined to α-type variables which obey the Onsager relation:

$$L_{jk} = L_{kj} \quad (3)$$

As pointed out by Prigogine,[2] the second law of thermodynamics requires that the total entropy production within any macroscopic portion of a system be positive or zero. However, it is not necessary that every *process* lead to positive entropy production. One driving process having a sufficiently high rate of positive entropy production can carry a coupled process along a nonspontaneous path. A necessary, though not sufficient, condition for this behavior is negative values of some of the L_{jk}.

It is known that active transport in biological systems is driven by a chemical reaction, the hydrolysis of adenosine triphosphate. However, a chemical reaction occurring in an isotropic system is a scalar quantity, whereas transport across a membrane is of vector character. Hence if a chemical reaction is to drive a transport process, the Curie–Prigogine theorem (which states that coupled processes in isotropic systems must have the same tensorial character) requires that the active transport system have some inherent anisotropy. This has been achieved in our model systems by binding catalytic sites to the membrane in an asymmetric manner with respect to its thickness (the direction of transport). Thus the membrane is not simply a partially permeable barrier, but it furnishes a spatial framework for an asymmetric distribution of catalytic sites, thereby causing the rate of a chemical reaction to vary from point to point through the membrane thickness.

We selected hydrolysis reactions for this initial study, a choice motivated primarily by the ease of analysis of reactants and products. The base membrane material is regenerated cellulose, and we have investigated both enzyme and acid-catalyzed hydrolysis reactions. The time course of the reaction was monitored by analysis, and a study was made of the osmotic behavior of reactive solutions separated by asymmetric catalytic membranes. An analytical description of the various processes occurring in such systems is developed for the interpretation of these experimental observations.

I. Procedures

(A) Membrane Preparation. The first of the two systems studied is the α-chymotrypsin-catalyzed hydrolysis of ethyl *N*-acetyl-L-tyrosinate (ET) to yield *N*-acetyl-L-tyrosine (T):

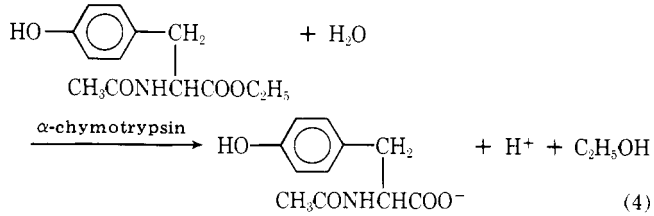

(4)

The active membrane was prepared by a two-step process. First, regenerated cellulose (American Viscose Division, Type 300), which had been conditioned to an equivolume mixture of acetone and water, was treated with 2-amino-4,6-dichloro-*S*-triazine to attach a "spacer". Next, the resulting film was washed and immediately treated with α-chymotrypsin at pH 8.8. Reaction with the triazine could be monitored by the infrared bands at 800 and 1460 cm^{-1}, while the attached enzyme gave an additional absorption at 1500 cm^{-1}. The resulting membrane has the following schematic structure:

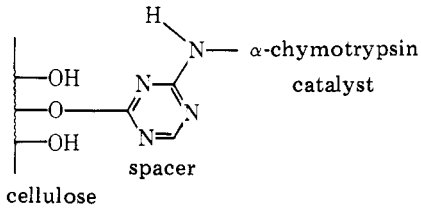

The specific activity of each membrane was determined by following the reaction of ET at pH 8 using a pH stat. The solvent was a phosphate buffer (5.3×10^{-3} M Na_2HPO_4 and 9.5×10^{-3} M NaH_2PO_4 containing 0.3 M NaCl and 7.5 vol % dioxane). The number of μmol of enzyme per cm^2 ranged from 0.008 to 0.04, indicating the sibstitution of fewer than one cellulose hydroxyl group per thousand. This small implantation level may be partially due to the large size of the α-chymotrypsin molecule. The same data yielded values for the zero-order rate constant, k_0, ranging from 0.5 to 1 s^{-1}. This is considerably smaller than the value 193 s^{-1} reported by Cunningham and Brown[3] and Bender[4] for α-chymotrypsin in solution at pH 7.9. This difference could be partly due to a lower pH in the active membrane than that of the external solution. Bender and co-workers[5] have shown that k_0 decreases with decreasing pH. Goldman, Kedem, and Katchalski[6] found a difference of 2–3 pH units exists across a 200–300 μm membrane containing papain during the hydrolysis of the ethyl ester of benzoyl-L-arginine. Further, Kay and Lilly[7] observed that k_0 for the hydrolysis of ET by α-chymotrypsin immobilized on cellulose-base pellets decreased about two orders of magnitude when the pH was decreased by 3 units. On the other hand, the difference may partially reflect inactivation of the enzyme, since we observe a further dicrease in the specific activity of the enzymic membranes during storage in a refrigerator. Asymmetric composites of one active film of thickness 82 μm and two untreated films (245 μm total composite thickness) were used for the studies to be described below.

The second reaction investigated is the acid-catalyzed hydrolysis of triethoxymethane (TEM):

$$HC(OC_2H_5)_3 + H_2O \xrightarrow{H^+} HCOOC_2H_5 + 2C_2H_5OH \quad (5)$$

Wet regenerated cellulose was conditioned to dry benzene and treated with oxalyl chloride in dry benzene containing pyridine, and the pendent acid chloride groups were hydrolyzed with hot water. The resulting membrane has the following schematic structure:

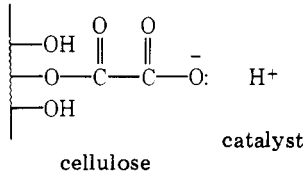

Implantation of carboxyl groups could be verified by the appearance of infrared bands at 1720, 2500 and 3000 cm^{-1}, and the number of moles of COOH per cm^2, as determined by titration, ranged from 0.2 to 70 (full substitution). The degree of substitution increased with reaction time, but for a given reaction time, the specific activity decreased with the age of the film prior to treatment. The active films averaged 80 μm in thickness, and each of these was backed with three layers of untreated cellulose (each 70 μm in thickness) to produced an asymmetric composite film of total thickness 290 μm. Acetone containing a small amount of water was used as the solvent for the hydrolysis reaction.

(B) Analytical and Osmotic Measurements. The osmotic behavior was investigated at 30 °C by clamping a composite membrane in a Stabin high-speed osmometer and filling both compartments with the same reactant solution. Since the volumes of the inner and outer compartments of the osmometer are different, separate runs were made with the active side of the membrane facing each compartment. The procedure used was to follow simultaneously the time course of the osmotic pressure and the concentrations of reactants and/or products as the reaction proceeded by withdrawing samples for analysis. While this procedure offers certain advantages, it has the disadvantage that neither compartment could be stirred mechanically. Further, withdrawal of a sample required termination of the osmotic measurements, so the same initial conditions were duplicated numerous times and the experiment was terminated by sampling after different time intervals.

The concentration of *N*-acetyl-L-tyrosine produced during the enzymatic hydrolysis was determined by pH measurement using a calibration curve constructed from solutions of known concentration of this product in the same buffer. The concentrations of all species in the acid-catalyzed reaction were determined by gas chromatography using a Poropak Q column. The precision was poorest for triethoxymethane and ethyl formate. The poorer result for the latter can be explained by the fact that its peak was located on the trailing edge of the large acetone (solvent) peak.

Permeability constants and reflection coefficients were determined by osmotic measurements of solutions of individual reactant or product. Data were obtained in most cases for both catalytic membranes and untreated cellulose. The permeability constants for the solutes were independently determined by the method of Yasuda, Lamaze, and Peterlin[8] using Leonard–Bluemle cells. In this case the membrane separates compartments of equal volume containing stirred solution and solvent, and the solute concentration is followed by withdrawing successive aliquotes after different periods of time. Ultraviolet spectroscopy was used to monitor the concentration of ester in the enzyme system, and the other analytical procedures were as described above.

Experimental Section

(A) Reflection Coefficients. The behavior of membranes toward partially permeable solutes has been considered by Staverman[9] and more recently by Katchalsky and Curran.[10] The latter authors have shown that the dissipation factor, $\Phi = T(d_iS/dt)$, for a system exhibiting both solute diffusion and osmotic flow can be expressed as:

$$\Phi = J_P P + J_D \pi^* \quad (6)$$

where P is the applied hydrostatic pressure, J_P and J_D are the flows of solution and solute (relative to that of the solvent), and $\pi^* = -\Delta\mu_1/\bar{V}_1$ is the "ideal" osmotic pressure. In the latter expression $\Delta\mu_1$ is the difference in chemical potential of solvent across the membrane and $\bar{V}_1$ is the partial molar volume of the solvent in the solution. The linear phenemenological equations corresponding to this formulation are:

$$J_P = L_P P + L_{PD}\pi^* \quad (7a)$$

$$J_D = L_{DP} P + L_D \pi^* \quad (7b)$$

Hence, if an osmotic experiment with partially permeable solutes is followed until the hydrostatic pressure attains its maximum value ($J_P = 0$), then:

$$P_{J_P=0} = -(L_{PD}/L_P)\pi^* \quad (8)$$

The ratio $-(L_{PD}/L_P)$ was designated as the reflection coefficient by Staverman and denoted by the symbol σ. Evidently the maximum hydrostatic pressure will only equal the ideal osmotic pressure if $\sigma = 1$, which corresponds to completely semipermeable behavior of the membrane toward the solute. If the solution contains several solutes, the solution flow can be expressed as:

$$J_P = L_P(P - \sum_i \sigma_i \pi^*) \quad (9)$$

The foregoing discussion indicates that mathematical description of

a system involving partially permeable solutes will require a knowledge of three parameters, L_P, L_D, and σ_i (or their equivalents), for each partially permeable component of the system.

The differential equation for the hydrostatic pressure given by Schulz and Kuhn[11] may be written in a slightly more generalized form:

$$dP_t/dt = -\lambda_1(P_t - \sigma\pi_t^*) \quad (10)$$

where P_t is the hydrostatic pressure developed at time t. If an experiment is performed with no concentration difference across the membrane, and one simply follows the decay of an initial hydrostatic pressure, then $\pi_t^* = 0$ for all t and eq 10 can be integrated to yield:

$$P_t = P_0 \exp(-\lambda_1 t) \quad (11)$$

which offers a procedure for evaluating the constant λ_1 characterizing the permeability of the membrane toward the solution. On the other hand, if a gradient of partially permeable solute exists across the membrane, then both P_t and π^* will vary with time. We stipulate that the final equilibrium value of the ideal osmotic pressure will be π_∞^*, so that the decrease of the ideal osmotic pressure due to transfer of the partially permeable solute across the membrane is given by:

$$\pi_t^* = \pi_\infty^* + (\pi_0^* - \pi_\infty^*) \exp(-\lambda_2 t) \quad (12)$$

where π_0^* is the value of the ideal osmotic pressure at time $t = 0$ and λ_2 characterizes the permeability of the membrane toward that solute. Substitution of this relation for π_t^* into eq 10 produces:

$$dP_t/dt + \lambda_1 P_t = \lambda_1\sigma\pi_\infty^* + \lambda_1\sigma(\pi_0^* - \pi_\infty^*) \exp(-\lambda_2 t) \quad (13)$$

It will be assumed that $\lambda_1 \gg \lambda_2$. Hence, if the initial conditions are selected so that $P_0 = 0$, the initial slope of a plot of P_t vs. t should be $\lambda_1\sigma\pi_0^*$, and if π_0^* is known this experiment, in conjunction with the one described above, permits an evaluation of the reflection coefficient σ.

Equation 13 may be solved using $\exp(-\lambda_1 t)$ as an integrating factor. Application of the boundary condition $P_0 = 0$ when $t = 0$ then gives:

$$P_t = P_0 e^{-\lambda_1 t} + \sigma\pi_\infty^* + \frac{\lambda_1\sigma(\pi_0^* - \pi_\infty^*)}{\lambda_1 - \lambda_2}(e^{-\lambda_2 t} - e^{-\lambda_1 t}) \quad (14)$$

We may assume that, at some sufficiently long time t', the term $\exp(-\lambda_1 t')$ will become arbitrarily small. Replacement of $\sigma\pi_\infty^*$ by P_∞ then yields:

$$P_t - P_\infty = \frac{\lambda_1\sigma(\pi_0^* - \pi_\infty^*)}{\lambda_1 - \lambda_2} e^{-\lambda_2 t} \quad (15)$$

Hence, for any time $t'' > t'$:

$$\ln\left(\frac{P_t'' - P_\infty}{P_t' - P_\infty}\right) = -\lambda_2(t'' - t')$$

and λ_2 may be evaluated from the slope of the indicated plot of the long-time data.

Turning to the treatment of permeation data, the difference, ΔC_t, of solute concentration in the two compartments at time t obeys the relation:

$$(\Delta C_{t_2}/\Delta C_{t_1}) = \exp[-\lambda_2(t_2 - t_1)] \quad (16)$$

and the permeation constant, D', is given by:

$$D' = (Vd/2A)\lambda_2 \quad (17)$$

where V is the volume of each compartment, and d and A are the thickness and area, respectively, of the membrane.

Equations 15 and 17 indicate that the permeation constant D' can be evaluated independently from the permeation cell measurements and from the long-time osmometer response. These two procedures yielded similar results when acetone was the solvent but for aqueous solutions much larger values from the osmotic data than from the permeation cell. Part of this difference may arise from difficulties in the osmotic measurements owing to large surface tension of water. Due to this uncertainty we were unable to obtain reliable values of λ_1 and σ for the enzyme membrane system. Table I gives the experimentally determined values of λ_2 and σ and the permeation constants D' and D'' for the catalytic and untreated membranes, respectively. The right-most column lists an estimate of the diffusion constant D of solute in solution, based upon the viscosity and dimensions of the solute molecules as viewed end-on.

(B) Concentrations of Reactants and Products. The enzyme-catalyzed reaction yielded products at a constant rate over a 5–6-h period, as expected for a zeroth-order reaction, while the analytical

Table I
Reflection, Permeation, and Diffusion Constants

(A) Enzyme-Catalyzed System

Solute	$10^6D'$	$10^6D''$	10^5D
ET		1.0	0.7
T	1.5	1.6	0.8
C_2H_5OH			1.6

B. Acid-Catalyzed System

Solute	$10^3\lambda_1$	$10^3\sigma$	$10^6D'$	$10^6D''$	10^5D
TEM	0.7	3	4	9	2
H_2O	4.3	0.3	10.5	12	7
$HCOOC_2H_5$	6.2	0.4	8	16	4
C_2H_5OH	3.2	0.8	7	8	4

results for the acid-catalyzed system confirmed the stoichiometry indicated in eq 5. A more quantitative interpretation of the experimental results will be based upon the theroretical treatment of asymmetric membrane systems which appears in the Appendix.

We consider first the zeroth-order enzyme catalysis. The derivative with respect to time of eq 47 in the Appendix gives for the rate of change of product concentrations $[P_L]$ and $[P_R]$ in the left and right compartments:

$$V_L\, d[P_L]/dt = (X_{1P} + X_{2P} + l)^{-1}[\nu_P k_0[E_0]Al(l/2 + X_{2P}) + D_P'(K_{1P}/K_{2P})(e^{-K_{2P}t} - 1)] \quad (18a)$$

$$V_R\, d[P_R]/dt = (X_{1P} + X_{2P} + l)^{-1}[\nu_P k_0[E_0]Al(l/2 + X_{1P}) - D_P'(K_{1P}/K_{2P})(e^{-K_{2P}t} - 1)] \quad (18b)$$

In each equation the first term arises from flow of product into that compartment due to reaction within the membrane, while the second term refers to the diffusion of product between compartments driven by the different product concentrations in the two compartments. There is initially no product in either compartment, so these equations can be simplified for short times by neglecting the diffusion term. We will adopt the convention that the active side of the membrane always faces the left compartment (which may be the inner or outer compartment of the osmometer). We further designate the arrangement in which the active side of the membrane faces the outer compartment with a prime, so that $V_L = V_R' = V_I$ and $V_R = V_L' = V_O$, where V_I and V_O are the volumes of the inner and outer compartments, respectively. The initial rates of change of product concentration are found to obey the following relationships:

$$\frac{d[P_L]/dt}{d[P_L']/dt} = \frac{d[P_R']/dt}{d[P_R]/dt} = \frac{V_R}{V_L} \quad (19)$$

$$\frac{V_L(d[P_L]/dt)}{V_R(d[P_R]/dt)} = \frac{V_R(d[P_L']/dt)}{V_L(d[P_R']/dt)} = \frac{l/2 + X_{2P}}{l/2 + X_{1P}} \quad (20)$$

$$V_L(d[P_L]/dt) + V_R(d[P_R]/dt) = V_R(d[P_L']/dt) + V_L(d[P_R']/dt) = \nu_P k_0[E_0]lA \quad (21)$$

For the enzyme-catalyzed hydrolysis the observed initial rates are $d[P_L]/dt = 7.5 \times 10^{-10}$, $d[P_L']/dt = 5.8 \times 10^{-11}$, $d[P_R']/dt = 4.2 \times 10^{-10}$, and $d[P_R]/dt = 3.8 \times 10^{-11}$ mol cm^{-3} s^{-1}. Substitution of the first pair into eq 19 yields $V_R/V_L = 13$, while the second pair gives 14 for the same ratio. These are smaller than the actual ratio of outer and inner volumes, 22, probably arising from nonuniform concentration in the (larger) outer compartment due to lack of stirring. If we adopt the average of the former values, $V_R/V_L = 13.5$, eq 20 furnishes the same value for the membrane asymmetry factor, $(l/2 + X_{2P})/(l/2 + X_{1P}) = 1.85$, for both ratios of rates. Calculation of this ratio according to eq 30 involves the thickness, δ, of the unstirred layers, which is difficult to estimate. As a crude approximation we assign δ as the depth of the grooves in the metal plates clamping the membranes, 3.8×10^{-2} cm. The additional values $l = 1.64 \times 10^{-2}$ cm, $D_P = 8 \times 10^{-6}$, $D_P' = 1.6 \times 10^{-6}$, and $D_P'' = 1.6 \times 10^{-6}$ cm s^{-1} then produce $X_{1P} = 7.1 \times 10^{-3}$ and $X_{2P} = 22.5 \times 10^{-3}$ cm, so that $(l/2 + X_{2P})/(l/2 + X_{1P})$ is calculated to be 2.0. Considering the uncertainties in several of the parameter values, the agreement with the experimental value, 1.85, is quite reasonable. Taking $V_L = 10$ cm^3 (actual) and $V_R = 135$ cm^3, eq 21 yields for $\nu_P k_0[E_0]lA$ the values 1.15×10^{-8} and 1.20×10^{-8} mol s^{-1}. Since $\nu_P = 1$, and from membrane specific activity data $[E_0] = 3.9 \times 10^{-8}$ mol cm^{-2}, the average of these values gives for the zero-order rate constant $k_0 = 0.034$ s^{-1}. This is significantly smaller than $k_0 = 0.52$ s^{-1} measured shortly after preparation of the membranes, indi-

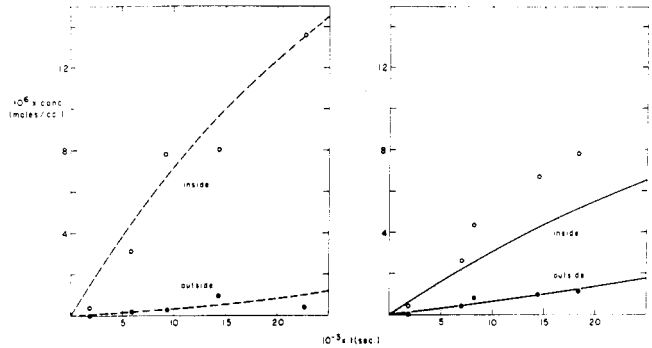

Figure 1. Concentration in the inside and outside compartments of the product, *N*-acetyl-L-tyrosine, vs. time calculated for the active side of the enzime membrane facing the inside (dashed) and outside (full curves).

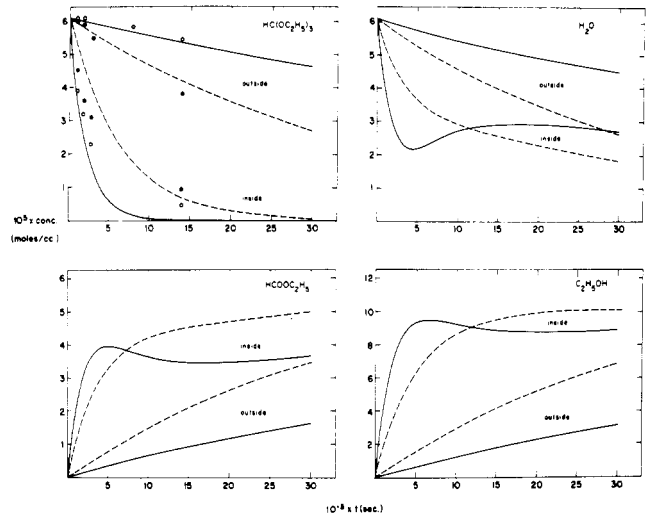

Figure 2. Calculated concentrations of reactants (above) and products (below) for the hydrolysis of triethoxymethane with the active side of the acid membrane facing the inside (full curves) and outside (dashed).

cating that the activity of the bound enzyme deteriorates with time, despite the fact the membranes were stored under buffer solution in a refrigerator.

We next turn to the initial behavior of the acid-catalyzed hydrolysis of triethoxymethane, which will be treated as a pseudo-first-order reaction. Differentiation of eq 52a and 52b produces the following relations for the rate of consumption of reactant:

$$-V_L(d[S_L]/dt) = \alpha A D_S'[(1 + X_{1S}'X_{2S}') + (X_{1S}' + X_{2S}') \coth \alpha l]^{-1} \times \{[S_L](\tanh (\alpha l/2) + X_{2S}') - ([S_R] - [S_L])/\sinh \alpha l\} \quad (22a)$$

and

$$-V_R(d[S_R]/dt) = \alpha A D_S'[(1 + X_{1S}'X_{2S}') + (X_{1S}' + X_{2S}') \coth \alpha l]^{-1} \times \{[S_R](\tanh (\alpha l/2) + X_{1S}') + ([S_R] - [S_L])/\sinh \alpha l\} \quad (22b)$$

The first term in the curly brackets represents the rate of transport of reactant from the compartment to the active region of the membrane, while the second arises from diffusion of reactant between the compartments. Since initially the reactant concentration is the same in both compartments, the latter may be neglected for short times, producing the following reactions involving the initial rates of change of reactant concentration:

$$\frac{d \ln [S_L]/dt}{d \ln [S_L']/dt} = \frac{d \ln [S_R']/dt}{d \ln [S_R]/dt} = \frac{V_R}{V_L} \quad (23)$$

$$\frac{V_L(d \ln [S_L]/dt)}{V_R(d \ln [S_R]/dt)} = \frac{V_R(d \ln [S_L']/dt)}{V_L(d \ln [S_R']/dt)} = \frac{\tanh (\alpha l/2) + X_{2S}'}{\tanh (\alpha l/2) + X_{1S}'} \quad (24)$$

$$V_L(d \ln [S_L]/dt) + V_R(d \ln [S_R]/dt) = V_R(d \ln [S_R']/dt) + V_L(d \ln [S_L']/dt) = -\alpha A D_S'\{(1 + X_{1S}')^{-1} + (1 + X_{2S}')^{-1}\} \quad (25)$$

The observed initial slopes for the hydrolysis of triethoxymethane are d ln $[S_L]/dt = -4.4 \times 10^{-4}$, d ln $[S_R]/dt = -1.25 \times 10^{-5}$, d ln $[S_L']/dt = -3.0 \times 10^{-5}$, and d ln $[S_R']/dt = -2.5 \times 10^{-4}$. From eq 23 these give for V_R/V_L 15 and 20, both considerably smaller than the actual volume ratio, which in this case was 40. Again, this difference probably arises from failure to provide stirring. Introduction into eq 24 of the average of the former values, 17.5, and the experimental slopes yields for the membrane asymmetry factor the values 2.0 and 2.1. In the present case $\alpha l = 4.75$, so that tanh $(\alpha l/2)$ can be replaced by unity. Again, there is reasonable agreement between these values and that calculated using $\alpha = 680$ cm^{-1}, $\delta = 4 \times 10^{-2}$ cm, and values for the permeation and diffusion constants taken from Table IB, $(1 + X_{2S}')/(1 + X_{1S}') = 2.2$. The experimental values for the sums appearing in eq 25 are 6.5×10^{-3} and 7.6×10^{-3} cm s^{-1}, giving an average of 7.0×10^{-3} cm s^{-1}. This corresponds to $k_1 = 2.0$ s^{-1} for the pseudo-first-order rate constant. Hine[12] has quoted 5.4×10^2 L mol^{-1} s^{-1} for the second-order rate constant for decomposition of triethoxymethane. Concentrations calculated using this value were plotted as ln (C_t/C_0) vs. t. An average slope of the resulting curve gave an estimate, $k_1 = 1.7$ s^{-1}, for the corresponding pseudo-first-order rate constant, in reasonable agreement with the experimental value cited above.

The foregoing discussion has been restricted to the initial rates of change of product or reactant concentration when diffusion between the two compartments can be neglected. We now turn to the variation of concentration over longer periods of time. Figure 1 shows the time dependence of one product of the enzyme-catalyzed hydrolysis, *N*-acetyl-L-tyrosine, calculated according to eq 18a and 18b. Three of the four cases agree moderately well with the experimental values, the exception being the product concentration in the inner compartment when the active side of the membrane faces the outside. In making these comparisons one must bear in mind that each point represents a separate run, that the runs were performed over a period of time, and, finally, that different (though similar) membranes were used for the "active side in" and "active side out" series.

In Figure 2 are shown the analogous plots of reactant product concentrations for the pseudo-first-order hydrolysis of triethoxymethane as calculated according to eq 22a and 22b. The agreement is within the rather large uncertainty of the analytical data (shown only for TEM). Inspection of the calculated curves for water and the two products leads to an interesting observation. Due to the diffusion current, each compartment does not function independently as a source of reactants and sink for products. Hence, the concentrations need not vary monotonically with time and, in fact, do not do so when the active side of the membrane faces the smaller, inner compartment. Taking ethyl formate as an example, we expect an initial flow of product outward through both faces of the membrane. Because this flow is more rapid through the active face (facing the inside), and the inner compartment has the smaller volume, the concentration of products builds up more rapidly in the inner compartment. However, this large concentration difference drives a rapid diffusion between the compartments which unloads product from the inner compartment, even while the reaction continues. At a later time the concentration difference has diminished, the unidirectional net flow is replaced by a bidirectional flow, and the concentration of ethyl formate again increases with time in both compartments.

The behavior just cited suggests that, under appropriate conditions, asymmetric catalytic membrane systems might be capable of sustaining an oscillatory behavior of some reactants or products. Such behavior might have interesting implications with respect to excitable membranes. Jain[13] has reviewed a number of model membrane systems which exhibit oscillatory behavior. Two general comments concerning the systems studied here may be worth noting. Negative feedback can be easily provided if the activity of the catalyst decreases with increasing product concentration. The α-chymotrypsin system provides an example. One product is hydrogen ion, and Bender et al.[5] have shown that the rate constant for the dissociation of the enzyme–substrate complex, K_3, decreases with increasing hydrogen-ion concentration. Kay and Lilly[7] report that K_3 for the same hydrolysis reaction we have studied, but with α-chymotrypsin immobilized on cellulose-base pellets, decreases by more than a factor of 100 for a decrease in pH of 3 units. Secondly, a continuous source of reactant must be provided if the oscillations are to be sustained. Computer simulation using a model having these features did produce sustained oscillations of concentration.

(C) Predicted Osmotic Behavior. The hydrostatic pressure at

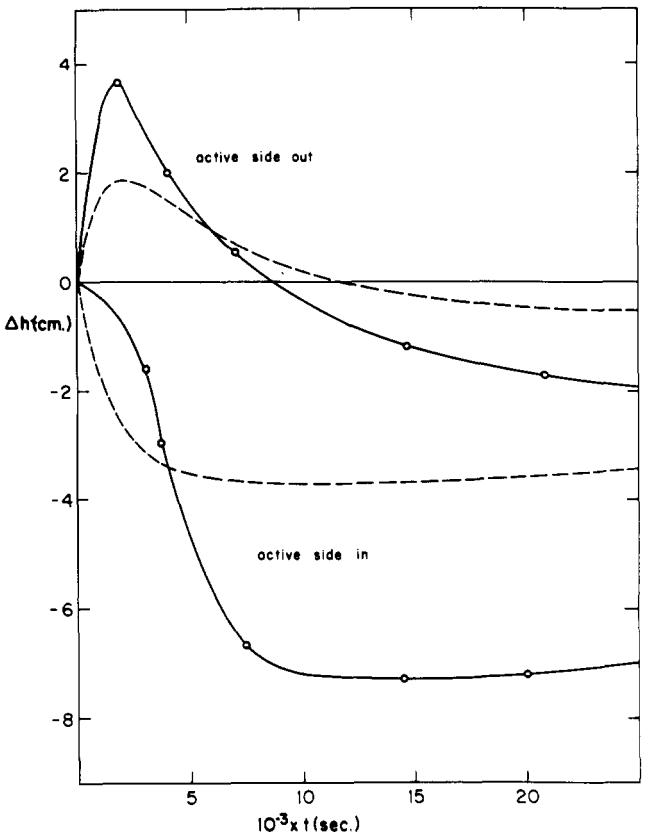

Figure 3. Observed (full curves) and predicted (dashed curves) osmotic responses for the hydrolysis of triethoxymethane with an asymmetric catalytic membrane.

any time may be calculated by computer from a knowledge of the concentrations of all species as a function of time and their reflection coefficients, σ_i, using a modification of eq 10:

$$dP/dt = \lambda_1(\pi - P) \tag{26}$$

where

$$\pi = RT \sum_i \sigma_i \Delta C_i / M_i \tag{27}$$

Here π is the effective osmotic pressure of the system containing several partially permeable solutes, and ΔC_i and M_i are the difference in concentration (g/cm^3) and molecular weight of solute i. One problem with this formulation is that the hydrostatic pressure is developed by a flow of solution across the membrane. According to Table I, λ_1 differs for solutions of the different permeable species, so that an average value must be used.

Since we were unable to obtain reliable values for the parameters of the enzyme membrane, our comparison with observed osmotic behavior must be restricted to that exhibited by the acid membrane. Figure 3 compares the predicted and observed time course of the hydrostatic pressure for triethoxymethane having an initial concentration 0.075 M. A negative response is observed when the active surface of the membrane faces the inside, and a positive peak occurs with the active face outside. The shapes of the predicted and observed curves are rather similar, although the magnitudes of the predicted extrema are too small by approximately a factor of 2. Due to the large reflection coefficient of triethoxymethane, and the stoicheometric coefficient of two for ethanol, these are the two most important species in determining the magnitude of the osmotic response. Errors in the reflection coefficients for these two species are one likely source of this discrepancy. On the other hand, the magnitudes of the negative pressure regions predicted for either membrane orientation could be increased by assuming a smaller value for the thickness, δ, of the unstirred layers. In this connection we note that Goldman, Kedem, and Katchalski[14] determined values for the thickness of the unstirred layer about a membrane directly exposed to solution which ranged from 0.0042 to 0.0066 cm. These values are considerably smaller than δ = 0.038 cm which are arbitrarily assigned for our clamped membranes.

In considering our osmotic observations from a qualitative point

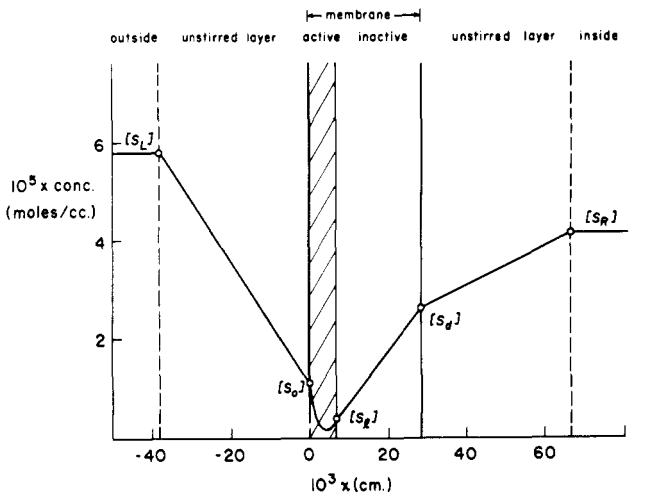

Figure 4. Calculated concentration profile of triethoxymethane at 2000 s with the active side of the membrane facing the outside.

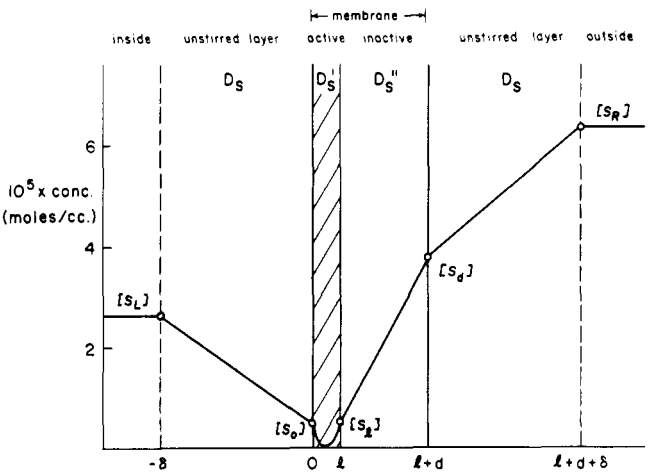

Figure 5. Parameters involved in treatment of the asymmetric membrane system. The profile shown is calculated for 2000 s of reaction with the active side of the membrane facing the inside.

of view, it should be noted that the ratio of the two compartment volumes is much larger than the membrane asymmetry factor (an effective value of 17.5 for the former and 2.1 for the latter). Thus, for either orientation of the membrane we expect the decrease in reactant concentrations, and the increase in product concentrations, should occur more rapidly in the inner compartment. This, in fact, does occur, as shown by reference to Figure 2. Further, in first approximation the sign of the osmotic response is determined by the difference in concentration of the reactant triethoxymethane. Hence, if the osmotic response were determined by the difference in concentration of the two solutions, a negative response would be predicted for either orientation of the membrane, contrary to observation. However, the osmotic response is determined by the concentration difference at the membrane *surfaces*. Due to the different path lengths for diffusion through the two surfaces, the concentration difference at the membrane surfaces can be opposite in sign to that of the external solutions. An example appears in Figure 4 for the active side of the membrane facing the larger, outer compartment. Once the reaction has begun, the concentration of reactant triethoxymethane is always larger in the outer compartment (left side). However, comparison of the concentration $[S_0]$ and $[S_d]$ at the membrane surfaces after 2000 s, which corresponds to the positive peak in Figure 3, shows a higher concentration at the inside surface, corresponding to a positive osmotic response. No such reversal occurs when the active side of the membrane faces the inner compartment (the profile calculated for 2000 s appears in Figure 5 in the Appendix).

Summary

The analysis presented at the outset indicated that, in order to be an effective agent for active transport, a membrane must

control a chemical reaction so that the reaction velocity varies through the membrane thickness. We have shown that composite catalytic membranes can be prepared which exhibit asymmetry, the rates of influx of reactants and efflux of products through the two membrane faces differing by approximately a factor of 2. A second source of asymmetry in our experiments arises from the different volumes of the two compartments separated by the membrane. Volume asymmetry is, of course, the general rule for biological membrane systems. This difference in volumes has important consequences, as can be seen from the different behavior observed with the active side of the membrane facing the inner or outer compartment. For example, with compartments of equal volume it is doubtful that one would observe a period of undirectional flow for water and the products of the triethoxymethane hydrolysis, or two types of osmotic response.

Our study provides no example in which a species is transported against the gradient of its chemical potential. We can, however, speculate how one might seek this behavior. Let us suppose that the diffusion of some nonreactive species, O, is coupled to that of one of the products of the triethoxymethane hydrolysis. We might expect that species to be "pumped" during the period when the product exhibits undirectional flow. Since ionic species are more likely to exhibit coupled transport, a model system involving redox reactions would be preferred.

Appendix

Barnes[15] was one of the early workers who considered the problem of diffusion through a membrane separating two stirred solutions of different concentration. Goldman, Kedem, and Katchalski[6] have given a methematical treatment for a system consisting of an asymmetric composite catalytic membrane separating compartments of infinite volume. Our treatment will be based upon a similar approach, but it will be necessary to modify the results of Goldman, Kedem, and Katchalski to allow for compartments of finite volume and unstirred layers at each exposed membrane surface.

Figure 5 illustrates a diagram of our asymmetric membrane system and identifies symbols for some of the important parameters. The membrane is a laminate consisting of an active region of thickness l and an inactive region of thickness d, and at each membrane surface there is an unstirred layer of thickness δ. The reactant will generally be indicated by the symbol S and the product by P. D is the diffusion coefficient in the unstirred layer, and D' and D'' are the permeation coefficients in the active and inactive layers, respectively. A subscript S or P designates whether the coefficient pertains to reactant or product. We designate the direction of transport as x and place the origin of this coordinate at the external surface of the active layer, as shown in Figure 5. The concentration in the left and right compartments (*e.g.*, $[S_L]$ and $[S_R]$) can be determined experimentally, while the corresponding concentrations $[S_0]$, $[S_l]$, and $[S_d]$ at the boundaries $x = 0$, $x = l$, and $x = l + d$, respectively, appear in the theoretical treatment, but are not accessible to direct measurement.

We begin with the assumption that, over short intervals of time, a steady state is attained within each volume element inside the active region of the membrane and that the concentration gradients of reactants and products are linear across the inactive membrane and the unstirred layers. Equating the fluxes across the boundaries at $x = -\delta$ and $x = 0$ and across the boundaries at $x = l$, $l + d$, and $l + d + \delta$ produces the following relations for reactant concentration:

$$[S_0] = [S_L] + X_{1S}\,(d[S]/dx)_{x=0} \tag{28a}$$

$$[S_l] = [S_R] - X_{2S}\,(d[S]/dx)_{x=l} \tag{28b}$$

$$[S_d] = [S_R] - X_{1S}\,(d[S]/dx)_{x=l} \tag{28c}$$

and for the product concentrations:

$$[P_0] = [P_L] + X_{1P}\,(d[P]/dx)_{x=0} \tag{29a}$$

$$[P_l] = [P_R] - X_{2P}\,(d[P]/dx)_{x=l} \tag{29b}$$

$$[P_d] = [P_R] - X_{1P}\,(d[P]/dx)_{x=l} \tag{29c}$$

where:

$$X_{1S} = \delta(D_S'/D_S) \tag{30a}$$

$$X_{1P} = \delta(D_P'/D_P) \tag{30b}$$

$$X_{2S} = \delta(D_S'/D_S) + d(D_S'/D_S'') \tag{30c}$$

$$X_{2P} = \delta(D_P'/D_P) + d(D_P'/D_P'') \tag{30d}$$

Within the active region of the membrane we assume that a steady state exists within each macroscopic volume element of the membrane, so that the following relations are obeyed:

$$d[S]/dt = D_S'\,d^2[S]/dx^2 - \nu_S V = 0 \tag{31a}$$

and

$$d[P]/dt = D_P'd^2[P]/dx^2 + \nu_P V = 0 \tag{31b}$$

where V is the reaction velocity and ν_S and ν_P are the stoichiometric coefficients for reactant and product, respectively. Equating the expressions for V leads to the differential equation:

$$d^2[P]/dx^2 = -\beta d^2[S]/dx^2$$

where $\beta = (\nu_P/\nu_S)(D_S'/D_P')$. Solution of this equation as a boundary value problem produces the relations:

$$(d[P]/dx)_{x=0} = ([P_l] - [P_0])/l + Y_0 \tag{32a}$$

$$(d[P]/dx)_{x=l} = ([P_l] - [P_0])/l + Y_l \tag{32b}$$

where:

$$Y_0 = \beta\{([S_l] - [S_0])/l - (d[S]/dx)_{x=0}\} \tag{33a}$$

$$Y_l = \beta\{([S_l] - [S_0])/l - (d[S]/dx)_{x=l}\} \tag{33b}$$

Substitution for $[P_l]$ and $[P_0]$ from eq 29 and solution of the resulting simultaneous equations leads to the desired relation for the product concentration gradients at the faces of the active region of the membrane:

$$(d[P]/dx)_{x=0} = (X_{1P} + X_{2P} + l)^{-1}\{[P_R] - [P_L] + lY_0 - X_{2P}(Y_l - Y_0)\} \tag{34a}$$

$$(d[P]/dx)_{x=l} = (X_{1P} + X_{2P} + l)^{-1}\{[P_R] - [P_L] + lY_l + X_{1P}(Y_l - Y_0)\} \tag{34b}$$

(A) Zeroth-Order Reaction. The gradients of reactants and products within the active region will depend upon the reaction kinetics. Zerner and Bender[16] have found that enzyme catalysis of specific substrates by α-chymotrypsin proceeds via the following mechanism:

$$E + S \underset{k_{-1}}{\overset{k_1}{\rightleftharpoons}} ES \xrightarrow{k_2} ES' \xrightarrow{k_3} E + P$$

where E represents the enzyme, S represents the substrate, ES and ES′ are intermediates, and P is the final product. Invoking the usual steady state approximation, and making use of the observation that $k_2 \gg k_3$,[15] one obtains for the reaction velocity, V:

$$V = \frac{k_3[E_0][S]}{(k_3/k_2)\{(k_{-1} + k_2)/k_1\} + [S]}$$

Further, Bender et al.[5] have shown that

$$k_3 = c_1/(1 + [H^+]/c_2)$$

where c_1 and c_2 are constants, so the final rate expression for α-chymotrypsin-catalyzed hydrolysis is:

$$V = \frac{c_1[E_0][S]}{(1 + [H^+]/c_2)\{(k_3/k_2)[(k_{-1} + k_2)/k_1] + [S]\}} \tag{35}$$

Unfortunately, use of this relation produces a nonlinear second-order differential equation for which no analytical solution could be found. Hence, we have resorted to the inferior zeroth-order representation:

$$V = k_0[E_0] \tag{36}$$

recognizing that k_0 for the membrane system will be substantially smaller than k_3 reported for enzyme catalysis in homogeneous solution at the same pH.

We now return to a consideration of the concentration of reactant within the active region of the membrane. Substitution of the latter relation into eq 31a, and solution of the resulting equation as a boundary value problem, gives:

$$[S_x] = [S_0] + \left\{\frac{[S_l] - [S_0]}{l} - \frac{\nu_S k_0[E_0]l}{2D_S'}\right\}x + \frac{\nu_S k_0[E_0]x^2}{2D_S'}$$

and differentiating once produces:

$$\frac{d[S]}{dx} = \frac{[S_l] - [S_0]}{l} + \frac{\nu_S k_0 [E_0]}{D_S'}\left(x - \frac{l}{2}\right) \quad (37)$$

It should be pointed out that the boundary conditions used above do not preclude the possibility that the minimum of the reactant concentration profile within the active region of the membrane might correspond to a negative concentration or might be located outside the range $0 \leq x \leq l$. If such a physically unrealistic behavior occurs, the boundary conditions employed above must be modified.

From eq 37 one can immediately write expressions for $(d[S]/dx)_{x=0}$ and $(d[S]/dx)_{x=l}$. Substitution for $[S_0]$ and $[S_l]$ from eq 28 then yields the following relations for the gradients of reactant at the two surfaces of the active layer:

$$(d[S]/dx)_{x=0} = (X_{1S} + X_{2S} + l)^{-1}\{[S_R] - [S_L] - (\nu_S k_0 [E_0] l/D_S')(X_{2S} + l/2)\} \quad (38a)$$

$$(d[S]/dx)_{x=l} = (X_{1S} + X_{2S} + l)^{-1}\{[S_R] - [S_L] + (\nu_S k_0 [E_0] l/D_S')(X_{1S} + l/2)\} \quad (38b)$$

The fluxes of reactant into the active region of the membrane from the left and right compartments are hence given by:

$$(J_S)_{x=0} = -D_S'(d[S]/dx)_{x=0} = (X_{1S} + X_{2S} + l)^{-1} \times \{\nu_S k_0 [E_0] l(l/2 + X_{2S}) + D_S'([S_L] - [S_R])\} \quad (39a)$$

$$-(J_S)_{x=l} = D_S'(d[S]/dx)_{x=l} = (X_{1S} + X_{2S} + l)^{-1} \times \{\nu_S k_0 [E_0] l(l/2 + X_{1S}) - D_S'([S_L] - [S_R])\} \quad (39b)$$

and the net flux of reactant into the active region is $(J_S)_{x=0} - (J_S)_{x=l} = \nu_S k_0 [E_0] l$. The same procedure may be followed, beginning with eq 31b, to obtain for the product gradients at the boundary of the active region the following expressions:

$$(d[P]/dx)_{x=0} = (X_{1P} + X_{2P} + l)^{-1}\{[P_R] - [P_L] + (\nu_P k_0 [E_0] l/D_P')(l/2 + X_{2P})\} \quad (40a)$$

$$(d[P]/dx)_{x=l} = (X_{1P} + X_{2P} + l)^{-1}\{[P_R] - [P_L] - (\nu_P k_0 [E_0] l/D_P')(l/2 + X_{1P})\} \quad (40b)$$

and for the product fluxes from the active region to the left and right compartments, respectively:

$$-(J_P)_{x=0} = D_P'(d[P]/dx)_{x=0} = (X_{1P} + X_{2P} + l)^{-1} \times \{\nu_P k_0 [E_0] l(l/2 + X_{2P}) - D_P'([P_L] - [P_R])\} \quad (41a)$$

$$(J_P)_{x=l} = -D_P'(d[P]/dx)_{x=l} = (X_{1P} + X_{2P} + l)^{-1} \times \{\nu_P k_0 [E_0] l(l/2 + X_{1P}) + D_P'([P_L] - [P_R])\} \quad (41b)$$

Thus far we have considered the behavior of the system in a steady state. Time dependence of the reactant and product concentrations is now introduced through the relations:

$$[S_L(t)] - [S(0)] = -(A/V_L)\int_0^t (J_S)_{x=0}\,dt \quad (42a)$$

$$[S_R(t)] - [S(0)] = (A/V_R)\int_0^t (J_S)_{x=l}\,dt \quad (42b)$$

and

$$[P_L(t)] - [P(0)] = -(A/V_L)\int_0^t (J_P)_{x=0}\,dt \quad (43a)$$

$$[P_R(t)] - [P(0)] = (A/V_R)\int_0^t (J_P)_{x=l}\,dt \quad (43b)$$

where A is the area of the membrane and V_L and V_R are the volumes of the left and right compartments. We have imposed the further condition that the initial concentration of reactant in the two compartments is identical, and the same is true for the product concentrations. Solution of the systems of equations for reactant and product concentration proceeds in a similar fashion, so this will only be exhibited in the latter case. Substitution for $(J_P)_{x=0}$ and $(J_P)_{x=l}$ from eq 41 produces:

$$[P_L(t)] - [P(0)] = (A/V_L)(X_{1P} + X_{2P} + l)^{-1} \times [\nu_P k_0 [E_0] l(l/2 + X_{2P})t - D_P'\int_0^t \{[P_L(t)] - [P_R(t)]\}\,dt] \quad (44a)$$

$$[P_R(t)] - [P(0)] = (A/V_R)(X_{1P} + X_{2P} + l)^{-1} \times [\nu_P k_0 [E_0] l(l/2 + X_{1P})t + D_P'\int_0^t \{[P_L(t)] - [P_R(t)]\}\,dt] \quad (44b)$$

The difference equation resulting upon substracting eq 44b from 44a can be solved immediately to yield:

$$[P_L(t)] - [P_R(t)] = (K_{1P}/K_{2P})(1 - e^{-K_{2P}t})$$

so that:

$$\int_0^t \{[P_L(t)] - [P_R(t)]\}\,dt = -(K_{1P}/K_{2P}^2)(1 - e^{-K_{2P}t}) + K_{1P}t/K_{2P} \quad (45)$$

where:

$$K_{1P} = [(\nu_P k_0 [E_0] lA)/(X_{1P} + X_{2P} + l)] \times [\{(l/2 + X_{2P})/V_L\} - \{(l/2 + X_{1P})/V_R\}] \quad (46a)$$

$$K_{2P} = [AD_P'/(X_{1P} + X_{2P} + l)][(V_R + V_L)/V_R V_L] \quad (46b)$$

Substitution of eq 45 into eq 44a and 44b produces the desired relations for the changes in product concentrations in the left and right compartments:

$$[P_L(t)] - [P(0)] = (A/V_L)(X_{1P} + X_{2P} + l)^{-1} \times [\nu_P k_0 [E_0] l(l/2 + X_{2P})t + D_P'(K_{1P}/K_{2P})\{(1/K_{2P})[1 - \exp(-K_{2P}t)] - t\}] \quad (47a)$$

$$[P_R(t)] - [P(0)] = (A/V_R)(X_{1P} + X_{2P} + l)^{-1} \times [\nu_P k_0 [E_0] l(l/2 + X_{1P})t - D_P'(K_{1P}/K_{2P})\{(1/K_{2P})[1 - \exp(-K_{2P}t)] - t\}] \quad (47b)$$

(B) First-Order Kinetics. Triethoxymethane is an ortho ester. According to March[17] it is readily hydrolyzed in the presence of acid through an S_N1 mechanism. Such S_N1 reactions obey pseudo-first-order kinetics in their initial stages because a slow reversible ionization is followed by a rapid combination of the intermediate carbonium ion with water. The reaction in homogenous solution is of second order; however, no analytical solution to the differential equation could be obtained for a second-order reaction. For the membrane reaction we may anticipate that the two reactants will be transported to the active region at fairly different rates, so that treatment of the hydrolysis as a pseudo-first-order process may furnish an adequate approximation. Hence, the velocity of the reaction at location x is represented as $V_x = k_1[S_x]$, where $[S_x]$ is the concentration of the rate-determining reactant at that location. Equation 31a then becomes:

$$D_S'\,d^2[S]/dx^2 = \nu_S k_1 [S] \quad (48)$$

Solution of this equation as a boundary value problem gives:

$$[S_x] = \{[S_l]\sinh \alpha x + [S_0]\sinh \alpha(l - x)\}/\sinh \alpha l \quad (49)$$

where $\alpha = (\nu_s k_1/D_S')^{1/2}$, so that

$$(1/\alpha)\,(d[S]/dx)_{x=0} = \{[S_l] - [S_0]\cosh \alpha l\}/\sinh \alpha l \quad (50a)$$

$$(1/\alpha)\,(d[S]/dx)_{x=l} = \{[S_l]\cosh \alpha l - [S_0]\}/\sinh \alpha l \quad (50b)$$

We may substitute for $[S_l]$ and $[S_0]$ from eq 28 and solve the resulting simultaneous equations to obtain:

$$\frac{1}{\alpha}\left(\frac{d[S]}{dx}\right)_{x=0} = \frac{[S_R] - [S_L](\cosh \alpha l + X_{2S}'\sinh \alpha l)}{(1 + X_{1S}'X_{2S}')\sinh \alpha l + (X_{1S}' + X_{2S}')\cosh \alpha l} \quad (51a)$$

$$\frac{1}{\alpha}\left(\frac{d[S]}{dx}\right)_{x=l} = \frac{[S_R](\cosh \alpha l + X_{1S}'\sinh \alpha l) - [S_L]}{(1 + X_{1S}'X_{2S}')\sinh \alpha l + (X_{1S}' + X_{2S}')\cosh \alpha l} \quad (51b)$$

where $X_{1S}' = \alpha X_{1S}$ and $X_{2S}' = \alpha X_{2S}$ are dimensionless quantities. From eq 42 with $(J_S)_{x=0} = -D_S'\,(d[S]/dx)_{x=0}$ and $(J_S)_{x=l} = -D_S'\,(d[S]/dx)_{x=l}$, we find for the reactant concentrations at time t:

$$[S_L(t)] - [S(0)] = (\alpha A D_S'/V_L)[(1 + X_{1S}'X_{2S}') + (X_{1S}' + X_{2S}')\coth \alpha l]^{-1}\int_0^t \{(1/\sinh \alpha l)([S_R] - [S_L]) - [S_L][\tanh(\alpha l/2) + X_{2S}']\}\,dt \quad (52a)$$

$$[S_R(t)] - [S(0)] = (\alpha A D_S'/V_R)[(1 + X_{1S}'X_{2S}') + (X_{1S}', + X_{2S}')\coth \alpha l]^{-1}\int_0^t \{(1/\sinh \alpha l)([S_R] - [S_L]) + [S_R][\tanh(\alpha l/2) + X_{1S}']\}\,dt \quad (52b)$$

and the total reaction velocity per cm^2, $\bar{V}_S$, is given by:

$$\bar{V}_S = (\alpha D_S'/\nu_S)[(1 + X_{1S}'X_{2S}') + (X_{1S}' + X_{2S}')\coth \alpha l]^{-1} \times \{([S_R] + [S_L]) \tanh (\alpha l/2) + X_{1S}'[S_R] + X_{2S}'[S_L]\} \quad (53)$$

If R represents a reactant which is not rate determining, then:

$$D_R' \, d^2[R]/dx^2 = \nu_R V \quad (54)$$

where ν_R is the corresponding stoicheometric coefficient. By the same procedure as above we may derive the following relations:

$$\left(\frac{d[R]}{dx}\right)_{x=0} = \frac{[R_l] - [R_0]}{l} + \gamma \left\{\frac{[S_l] + [S_0]}{l} + \left(\frac{d[S]}{dx}\right)_{x=0}\right\} \quad (55a)$$

and

$$\left(\frac{d[R]}{dx}\right)_{x=l} = \frac{[R_l] - [R_0]}{l} + \gamma \left\{\frac{[S_l] + [S_0]}{l} + \left(\frac{d[S]}{dx}\right)_{x=l}\right\} \quad (55b)$$

where $\gamma = (\nu_R/\nu_S)(D_S'/D_R')$. Substitution of the expressions:

$$[R_0] = [R_L] + X_{1R}\left(\frac{d[R]}{dx}\right)_{x=0} \quad (56a)$$

$$[R_l] = [R_R] - X_{2R}\left(\frac{d[R]}{dx}\right)_{x=l} \quad (56b)$$

where $X_{1R} = \delta D_R'/D_R$ and $X_{2R} = X_{1R} + dD_R'/D_R''$ produces the final relations:

$$\left(\frac{d[R]}{dx}\right)_{x=0} = \frac{[R_R] - [R_L] + lW_0 - X_{2R}(W_l - W_0)}{X_{1R} + X_{2R} + l} \quad (57a)$$

and

$$\left(\frac{d[R]}{dx}\right)_{x=l} = \frac{[R_R] - [R_L] + lW_l + X_{1R}(W_l - W_0)}{X_{1R} + X_{2R} + l} \quad (57b)$$

where:

$$W_0 = \gamma\{(1/l)([S_l] + [S_0]) + (d[S]/dx)_{x=0}\} \quad (58a)$$

$$W_l = \gamma\{(1/l)([S_l] + [S_0]) + (d[S]/dx)_{x=l}\} \quad (58b)$$

Acknowledgment. This work was partially supported under Grant HL-12157 from the National Institute of Health, Public Health Service. It is a pleasure to dedicate this work to Dr. Maurice L. Huggins who, over the years, has made significant contributions to our understanding of polymer solution thermodynamics.

References and Notes

(1) Address correspondence to this author.
(2) I. Prigogine, "Introduction to Irreversible Thermodynamics", 3rd ed, Interscience, New York, N.Y., 1967.
(3) L. W. Cunningham and C. S. Brown, *J. Biol. Chem.*, **221**, 287 (1956).
(4) M. L. Bender, *J. Am. Chem. Soc.*, **84**, 2583 (1962).
(5) M. L. Bender, G. E. Clement, F. J. Kézdy, and H. d'A. Heck, *J. Am. Chem. Soc.*, **86**, 3680 (1964).
(6) R. Goldman, O. Kedem, and E. Katchalski, *Biochemistry*, **7**, 4518 (1968).
(7) G. Kay and M. D. Lilly, *Biochim. Biophys. Acta*, **198**, 281 (1970).
(8) H. Yasuda, C. E. Lamaze, and A. Peterlin, *J. Polym. Sci., Part A-2*, **9**, 1125 (1971).
(9) A. Staverman, *Recl. Trav. Chim. Pays-Bas*, **70**, 344 (1951).
(10) A. Katchalsky and P. F. Curran, "Non-equilibrium Thermodynamics in Biophysics", Harvard University Press, Cambridge, Mass., 1967, p 119.
(11) G. V. Schulz and W. H. Kuhn, *Makromol. Chem.*, **29**, 220 (1959).
(12) J. Hine, *J. Am. Chem. Soc.*, **85**, 3239 (1963).
(13) M. K. Jain, "The Bimolecular Lipid Membrane: A System", Chapter 8, Van Nostrand-Reinhold, New York, N.Y., 1972.
(14) R. Goldman, O. Kedem, and E. Katchalski, *Biochemistry*, **10**, 165 (1971).
(15) C. Barnes, *Physics*, **5**, 5 (1934).
(16) B. Zerner and M. L. Bender, *J. Am. Chem. Soc.*, **86**, 3669 (1964).
(17) J. March, "Advanced Organic Chemistry: Reactions, Mechanisms and Structure", McGraw-Hill, New York, N.Y., 1968, p 306.

Molecular Relaxations in Partially Hydrogenated *cis*-1,4-Polybutadienes. A Guide to the Glass Transition Temperature of Amorphous Polyethylene

J. M. G. Cowie* and I. J. McEwen

Department of Chemistry, University of Stirling, Stirling FK9 4LA, Scotland.
Received April 11, 1977

ABSTRACT: A series of partially hydrogenated polybutadienes has been prepared by treating a sample of *cis*-1,4-polybutadiene with *p*-toluene sulfonhydrazide for varying lengths of time. The resulting polymers, which can be regarded as random copolymers of ethylene with acetylene, were examined by differential scanning calorimetry (DSC) and torsional braid analysis (TBA). The glass transition temperature (T_g) of amorphous polyethylene was estimated by plotting the T_g's of the copolymers, derived from DSC measurements, as a function of composition and extrapolating to 100% ethylene content. A value in the range 197–200 K was obtained using two extrapolation methods. Dynamic mechanical spectra exhibit a number of damping maxima for the copolymers, and attempts are made to identify these. The results suggest that the γ relaxation in polyethylene is not the glass temperature but is more likely to result from a crankshaft motion of short methylene sequences in the chain.

In spite of the vast amount of work reported on the relaxations observed in both linear and branched polyethylene, there is still no consensus on the precise temperature of the glass transition. Extensive reviews have been presented, most recently by Stehling and Mandelkern[1] and by Boyer[2] which highlight this problem, and each arrives at a different conclusion. It is now well established that polyethylene samples of medium crystallinity exhibit three major loss peaks in their dynamic mechanical spectra, at 145 ± 10 K, 240 ± 20 K and 340 ± 10 K, called respectively the γ, β, and α peaks. In high-density linear polyethylene the β peak tends to disappear and another damping maximum is found at temperatures of 390 ± 20 K called the α' peak.

Stehling and Mandelkern[1] have suggested that the glass temperature (T_g) for polyethylene is approximately 145 K and can be identified as the γ relaxation. This view is supported by Fischer and Kloos[3] from small-angle x-ray studies on linear polyethylene and by heat-capacity data reported by Beatty and Karasz.[4] From a study of the Raman spectra of rapidly quenched high-density polyethylene, Hendra et al.[5] have observed that the onset of crystallization takes place at temperatures near 190 K. They conclude that T_g must then lie near or below this temperature but were unable to identify a specific value. Boyer[1,6] has critically examined the evidence on which Stehling and Mandelkern base their conclusions and proposes instead that while the evidence supports the con-